Supplementary data

Dissecting Spatial Knowledge from Spatial Choice by Hippocampal NMDA Receptor Deletion

David M. Bannerman*, Thorsten Bus, Amy Taylor, David J. Sanderson, Inna Schwarz, Vidar Jensen, Øivind Hvalby, J. Nicholas P. Rawlins, Peter H. Seeburg* and Rolf Sprengel

*Correspondence: David.Bannerman@psy.ox.ac.uk (Phone: 0044-1865271426 Fax: 0044-1865310447) and Peter.Seeburg@mpimf-heidelberg.mpg.de (Phone: 0049-6221486495 Fax: 0049-6221486110)

10 Supplemental Figures

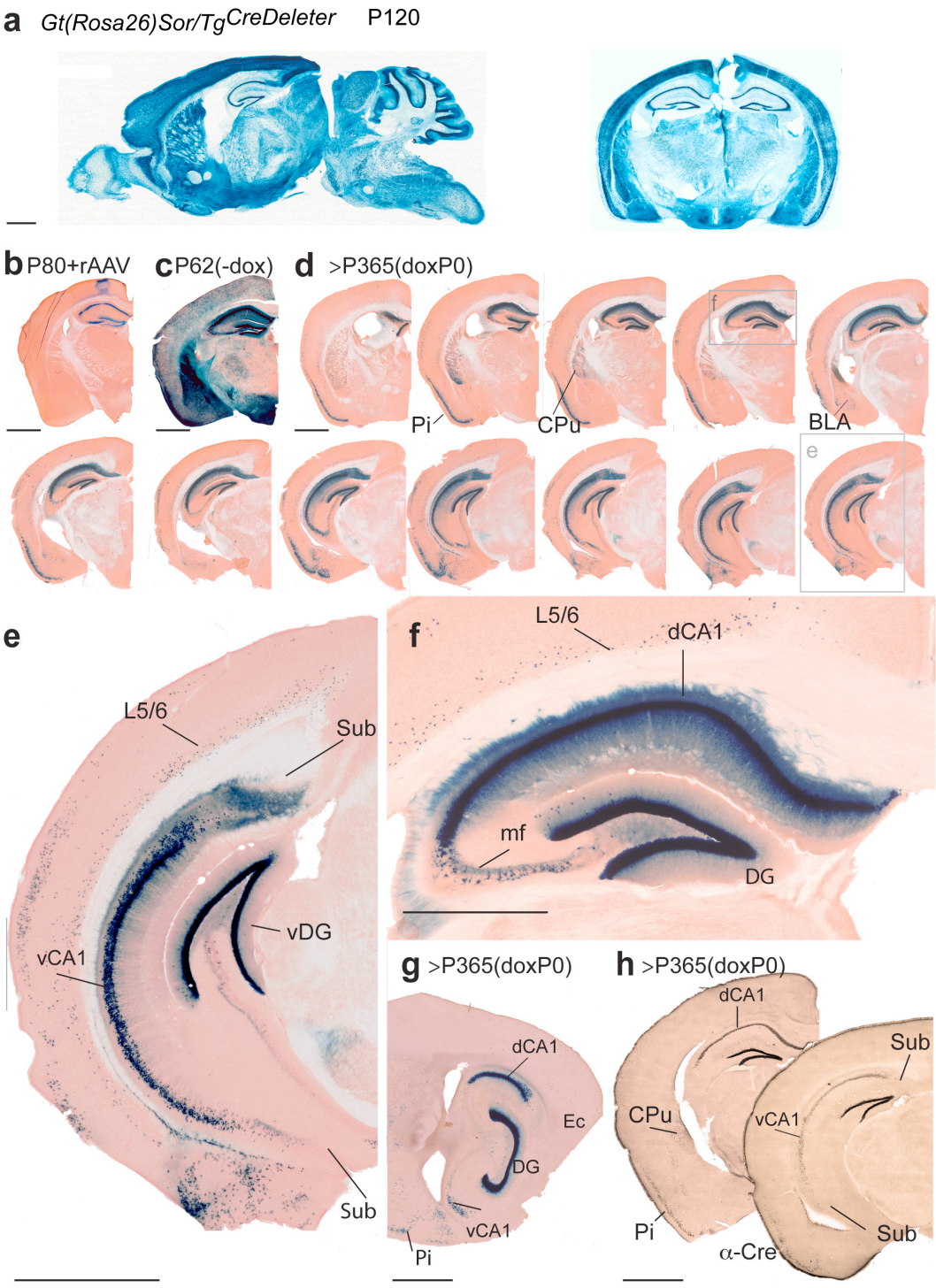

Supplementary Fig. 1. Cre activity can be monitored with high sensitivity in the brains of *Gt(Rosa)26Sor* mice. (**a**) After germ line deletion of the floxed stop cassette within the *Gt(Rosa26)Sor* locus, the lacZ reporter gene expression can be detected by X-Gal staining everywhere in the brain, indicating that the lacZ reporter gene can be expressed in all cells in the brain. (**b**) The Cre-accessibility of the *Gt(Rosa26)Sor* locus in mature neurons is demonstrated by rAAV-mediated, synapsin promoter-controlled Cre expression in the cortex of *Gt(Rosa)26Sor* mice that show Cre activated lacZ expression

(blue) in all cortical and hippocampal layers five weeks post injection. (**c**) Dox-naïve compound transgenic *Tg*$^{LC1/CN12}$*/Gt(Rosa)26Sor* mice have Cre-activated lacZ expression in many cortical and hippocampal cells. (**d**) In dox-suppressed *Tg*$^{LC1/CN12}$*/Gt(Rosa)26Sor* mice (dox treatment until P0) the Cre activity in cortical neurons and hippocampal CA3 is nearly completely abolished. As demonstrated by the 12 successive coronal brain sections (rostral to caudal), the activity is very strong in dorsal CA1 and to a lesser extent in ventral CA1. Magnified (**e**) ventral and (**f**) dorsal sections showed a reduced Cre activity in the ventral versus the dorsal CA1. The cortex shows sparse lacZ expressing cells in layer5/6 and to a higher extent in the piriform cortex (Pi, ~30% of layer II neurons) and caudate putamen (CPu). (**g**) Parasagittal sections show no Cre activity in the entorhinal cortex (Ec) (**h**). The Cre-immunostains confirmed the reduced Cre-expression in the ventral CA1 compared to the dorsal CA1. Sub., Subiculum; dCA1, dorsal CA1; vCA1, ventralCA1; mf, mossy fibers; P…, postnatal day; doxP0, animals were treated with dox until birth; Scale bars, 1mm.

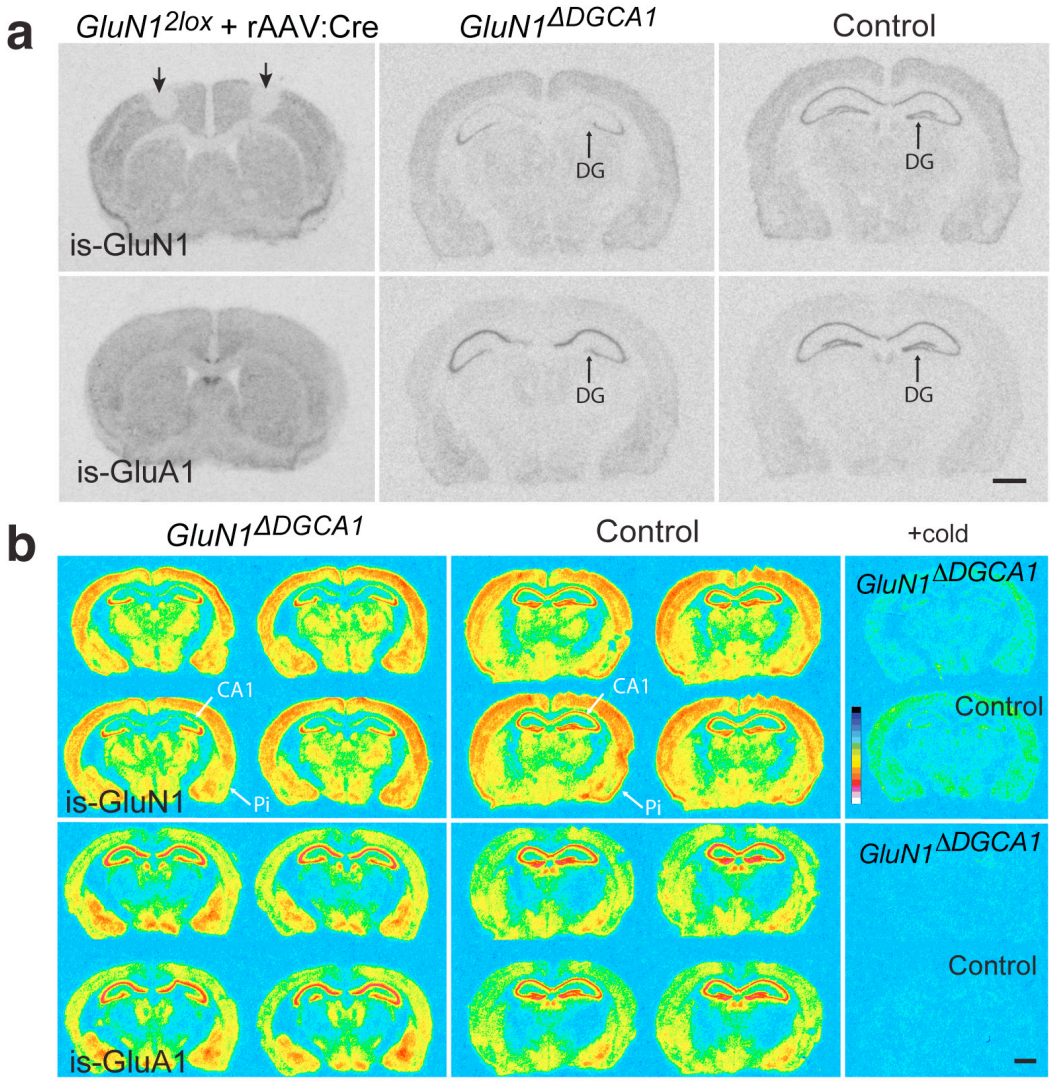

Supplementary Fig. 2. Cre-induced depletion of GluN1 mRNA can be visualized and quantified in brain sections of *GluN1*$^{\Delta DGCA1}$ mice. (**a**) Coronal brain slices after *in situ* hybridizations with antisense oligonucleotide probes recognizing GluN1 (is-GluN1) and GluA1 (is-GluA1) mRNA. (left) The rAAV-synapsin promoter-controlled Cre expression in the motor cortex of *GluN1*^{2lox} mice (2 month old) was detected by the specific loss of GluN1 mRNA in the virus-infected cortical areas (arrows) indicating that in cortical neurons the *Grin1*^{tm1rsp} alleles are accessible for Cre-mediated recombination. In *GluN1*$^{\Delta DGCA1}$ mice, older than one year, specific loss of GluN1 mRNA could be detected in CA1 and DG regions. The mRNA loss in the DG is, in part, non-specific due to loss of DG granule cells, as indicated by the strongly reduced GluA1 mRNA levels in the DG. (right) Age-matched Controls. Scale bar, 1 mm. (**b**) Semi-quantitative *in situ* hybridizations on serial brain sections as in (**a**) (middle and right) reveal specific loss of GluN1 mRNA in CA1, DG and piriform cortex (arrows), and no obvious differences in cortical GluA1 and GluN1 expression of Controls and *GluN1*$^{\Delta DGCA1}$ mice. The right panel shows the background signal of *in situ* hybridizations performed in the presence of a 20-fold excess of unlabeled (+cold) specific oligonucleotides. Pi, Piriform cortex; Calibration bar, 0 – 250 grey values; Scale bar, 1 mm.

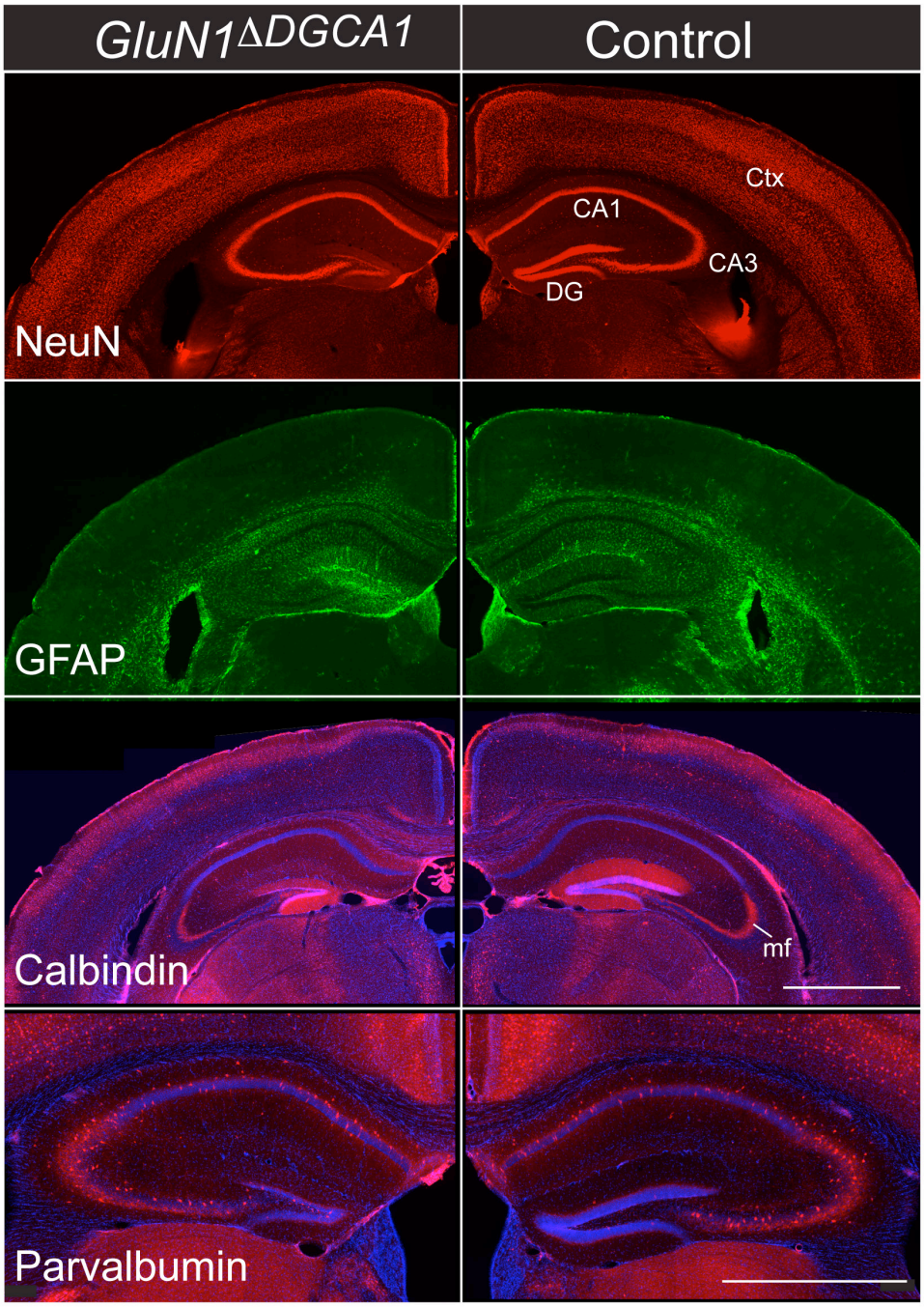

Supplementary Fig. 3. Alterations of neuronal markers can be detected only in the DG of *GluN1*$^{\Delta DGCA1}$ mice. The reduction of the DG volume was apparent in coronal brain sections from one-year old *GluN1*$^{\Delta DGCA1}$ mice, which had been used previously in the behavioral experiments. The reduced DG volume was accompanied by decreased numbers of NeuN positive granule cells and increased numbers of GFAP positive astrocytes in the DG. The mossy fiber (mf) projection visualized by Calbindin immunostains and the Parvalbumin positive interneurons were comparable between Controls and *GluN1*$^{\Delta DGCA1}$mice. In cortical areas (Ctx) the NeuN, GFAP and Calbindin expression had identical patterns between Controls and *GluN1*$^{\Delta DGCA1}$mice. Scale bar, 1mm.

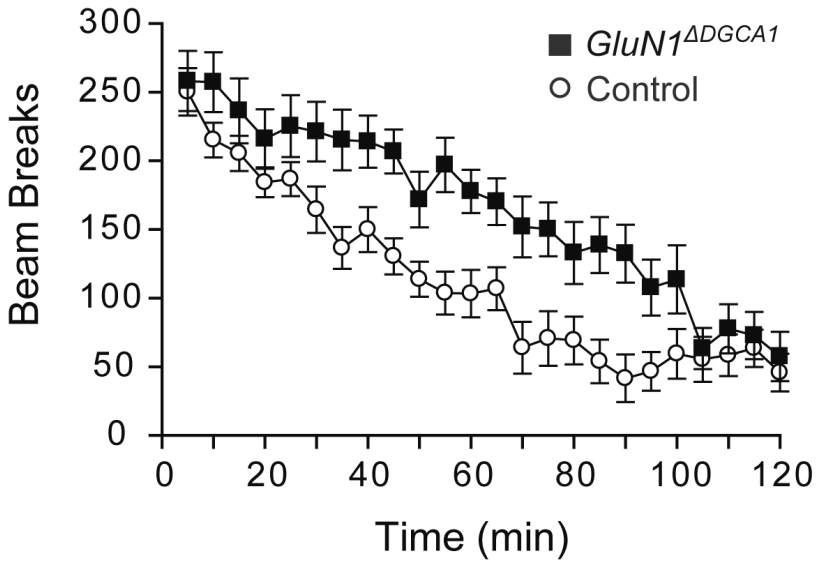

Supplementary Fig. 4. *GluN1*$^{\Delta DGCA1}$ mice exhibit locomotor hyperactivity in a novel environment. Spontaneous locomotor activity was measured in transparent plastic photocell activity cages (26 cm x 16 cm x 17 cm; with a ventilated lid). Two infrared photocell beams crossed the cage 1.5 cm above the floor, with each beam 7 cm from the center of the cage. Animals were placed singly into a cage and were left in a quiet room with the lights on for 2 h. The figure shows mean ± s.e.m. total beam breaks during 24 five-minute bins for Controls (white circles) and *GluN1*$^{\Delta DGCA1}$ mice (black squares). The total beam breaks made during the 2 h test were Controls = 2681 ± 270; *GluN1*$^{\Delta DGCA1}$ = 3968 ± 391; t (22) = 2.71; p = 0.01 (n = 12 per genotype; Age of the animals was 7 – 8 months).

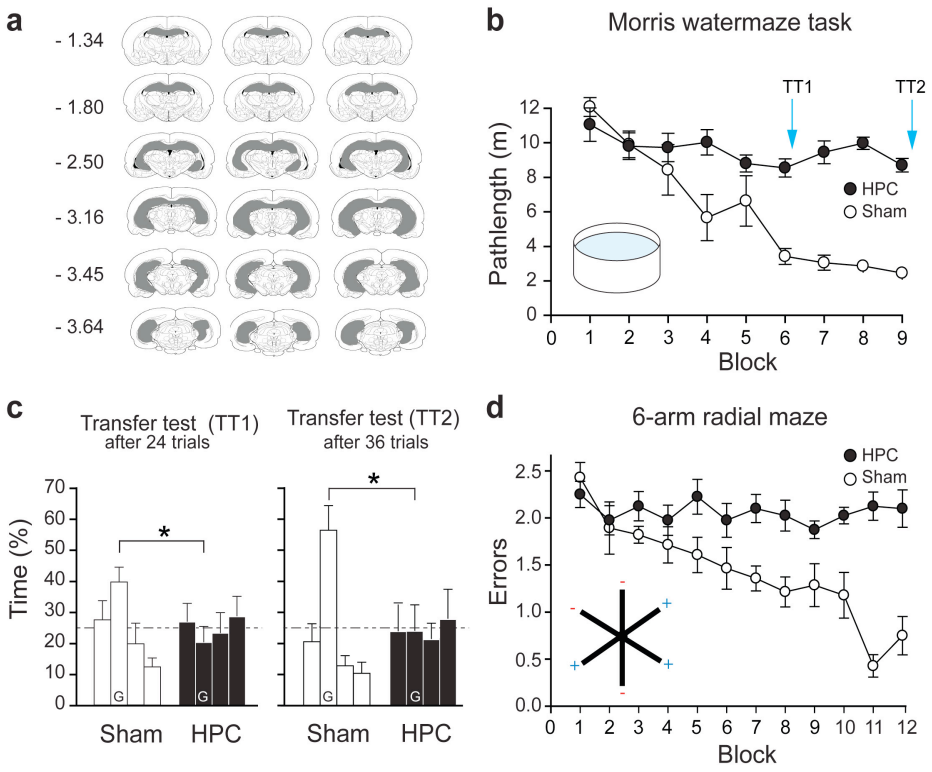

Supplementary Fig. 5. Spatial reference memory is hippocampus-dependent. To confirm the hippocampal dependency of the watermaze and radial maze tasks in our laboratory, male C57Bl6 mice with cytotoxic hippocampal lesions (HPC; n = 10) were compared to Sham operated controls (n = 7). (**a**) Reconstructions of brains from mice with hippocampal lesions showing minimum (left column), representative (middle column) and maximum (right column) extent of the damage. Grey indicates the areas of destruction and numbers at the left-hand side indicate approximate distance in millimeters posterior to bregma. (**b**) HPCs impair acquisition of the hidden escape platform version of the Morris watermaze task. Spatial reference memory was assessed as described for *GluN1*$^{\Delta DGCA1}$ mice and their Controls. Animals had no swim pre-training prior to the start of spatial testing. As expected, mice with hippocampal lesions were dramatically impaired and took longer pathlengths to find the platform during training (group - $F(1,15) = 34.69$; $p < 0.0001$, group x block interaction - $F(8,120) = 9.41$; $p < 0.0001$). The figure shows mean ± s.e.m. pathlengths of Sham and cytotoxic hippocampal lesioned mice during 9 days of acquisition training (4 trials/block). (**c**) On the seventh (24 h after spatial training trial 24) and tenth days of testing (24 h after spatial training trial 36), a probe trial was conducted. The platform was removed from the pool and the mice were allowed to swim freely for 60 s. Hippocampal lesioned mice exhibited no preference for the training quadrant and were significantly impaired relative to the sham animals (comparison of % time in the training quadrant; Sham vs. HPC; transfer test 1 – $t(15) = 2.72$; $p<0.05$, transfer test 2 – $t(15) = 2.64$; $p<0.05$) indicating a spatial memory impairment. The figure shows mean ± s.e.m. percentage time spent in each quadrant (adjacent left, Goal, adjacent right, opposite). Broken line: chance levels of performance. (**d**) HPCs impair acquisition of a spatial reference memory task on the 6-arm radial maze was assessed as described for *GluN1*$^{\Delta DGCA1}$ mice and their Controls. Whereas shams gradually reduced their spatial reference memory errors, the hippocampal lesioned animals made no improvement across blocks. ANOVA revealed main effects of group ($F(1,15) = 43.92$; $p < 0.0001$) and block ($F(11,165) = 5.70$; $p < 0.0001$), and a group by block interaction ($F(11,165) = 4.87$; $p<0.0001$). The figure shows mean ± s.e.m. number of spatial reference memory errors per trial (entries into unbaited arms) for Sham and HPC mice during 12 blocks of training (4 trials/block; maximum 3 errors per trial).

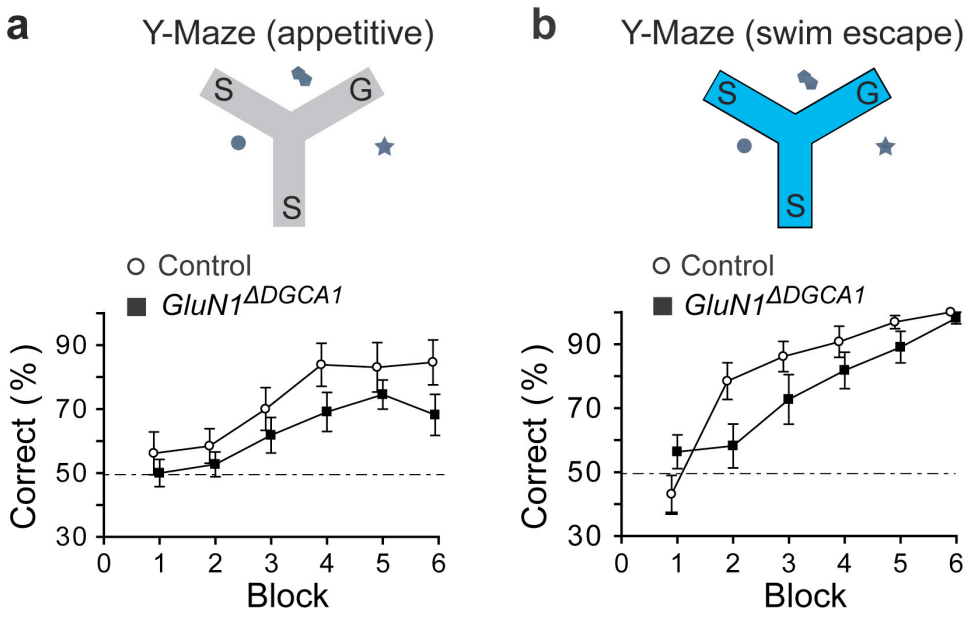

Supplementary Fig. 6. *GluN1*$^{\Delta DGCA1}$ mice are impaired on both appetitive and aversive (swim-escape) versions of the Y-maze spatial reference memory task. The top part of each figure depicts the Y-maze with two possible start arms (S) and a goal arm (G) which was in a constant location relative to the extramaze spatial cues, and contained either a food reward (appetitive version) or an escape platform (aversive version). **(a)** Controls (n = 12) and *GluN1*$^{\Delta DGCA1}$ mice (n = 12) were trained on an appetitively motivated, spatial reference memory task using an elevated Y-maze (10 trials per block). Acquisition was impaired in the *GluN1*$^{\Delta DGCA1}$ mice. ANOVA revealed a significant main effect of genotype ($F(1,22) = 7.06$; $p = 0.01$), a significant main effect of block ($F(5,110) = 14.69$; $p < 0.0001$), but no genotype by block interaction ($F < 1$; $p > 0.70$). Post-choice reinforcement trials during which the condensed milk reward was added to the food well only after the mouse had made a choice, confirmed that the animals were not locating the milk by virtue of its odor. The figure shows mean ± s.e.m. percent correct choices for Controls (white circles) and *GluN1*$^{\Delta DGCA1}$ mice (black squares). **(b)** Mice were also tested in a deep-water escape (aversive) Y-maze spatial reference memory task (5 trials per block). Previous work within this laboratory has confirmed that the swimming Y-maze task, like the appetitive Y-maze, is hippocampus-dependent. Like the appetitive version, acquisition of this aversively motivated, swim-escape spatial reference memory Y-maze task was impaired in the *GluN1*$^{\Delta DGCA1}$ mice compared to Controls (n = 12 per genotype). ANOVA revealed a main effect of block ($F(5,110) = 31.48$; $p < 0.0001$) and a significant genotype by block interaction ($F(5,110) = 3.19$; $p < 0.01$). Subsequent analysis of simple main effects confirmed that the *GluN1*$^{\Delta DGCA1}$ mice were significantly impaired during block 2 of testing ($F(1,22) = 5.22$; $p < 0.05$). There was no overall main effect of genotype ($F(1,22) = 2.57$; $p > 0.10$). The figure shows mean ± s.e.m. percent correct choices for Controls (white circles) and *GluN1*$^{\Delta DGCA1}$ mice (black squares) during the aversively motivated version of the Y-maze task.

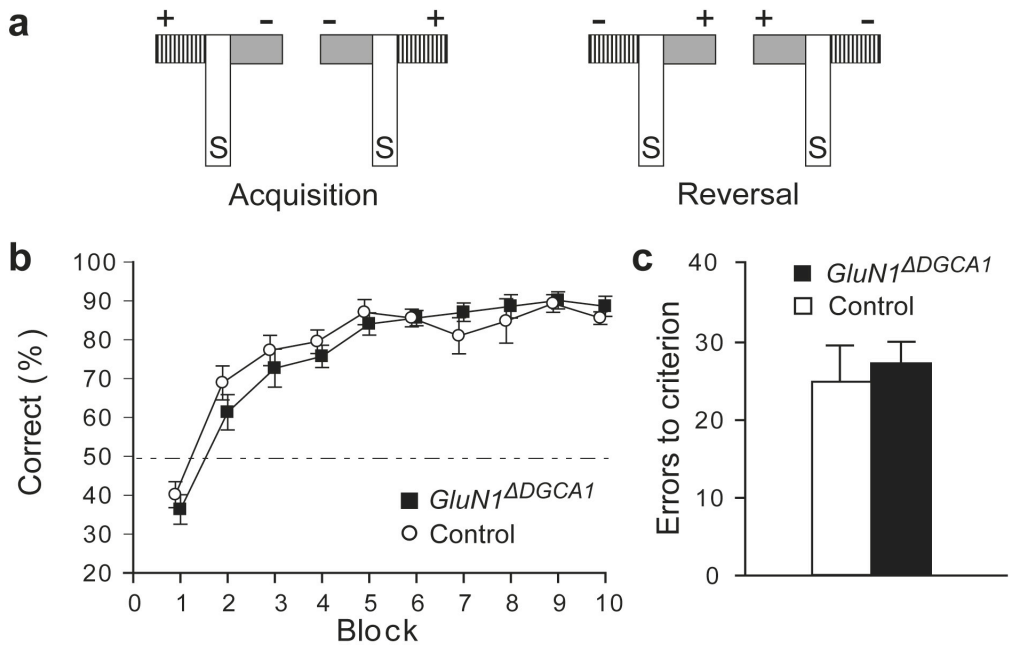

Supplementary Fig. 7. Preserved performance during reversal of an appetitively motivated, simple visual discrimination in *GluN1*$^{\Delta DGCA1}$ mice. (a) Non-spatial reversal; mice were first trained to associate a particular colored goal arm on the T-maze with a food reward as described for the appetitively motivated, simple visual discrimination**.** Mice received training blocks of 12 trials per day and during acquisition were trained to a criterion of 10 out of 12 correct choices (83.33% correct) on three consecutive days of testing. During acquisition 6 Controls and 6 *GluN1*$^{\Delta DGCA1}$ mice were trained that the grey insert was rewarded, and 5 of each genotype were trained that the black and white striped goal arm was rewarded. On the day after criterion was achieved by an individual mouse, the identities of the rewarded (+) and non-rewarded (–) goal arms were reversed for that animal. Thus, for an animal that had been trained that the black and white striped goal arm was rewarded during acquisition, the grey goal arm was now rewarded during reversal. During the reversal phase, mice were again trained to a criterion of 10 out of 12 correct choices (83.33% correct) on three consecutive days of testing. All mice were tested for a minimum of 10 days and a maximum of 16 days during reversal, irrespective of whether or not they had achieved criterion. As expected Controls and *GluN1*$^{\Delta DGCA1}$ mice acquired the simple visual discrimination task at the same rate (errors to criterion – $t < 1$; $p = 0.90$; data not shown). (**b**) Similarly, during reversal of this non-spatial task both Controls and *GluN1*$^{\Delta DGCA1}$ mice performed equivalently. Analysis of first choice accuracy on the 10 days of reversal testing that were completed by all of the animals revealed a significant main effect of block ($F(9,180) = 77.52$; $p < 0.0001$), but no main effect of genotype or genotype by block interaction (both $F \leq 1.01$; $p > 0.40$). A separate analysis of just the first 6 trials during day 1 of reversal also failed to reveal a group difference (% correct - Control = 31.8 ± 6.9; *GluN1*$^{\Delta DGCA1}$ = 27.3 ± 5.2; $t < 1$; $p = 0.60$). The figure shows mean ± s.e.m. percent correct choices in Controls (n = 11) and *GluN1*$^{\Delta DGCA1}$ mice (n = 11) across the 10 blocks of reversal testing (12 trials per block) that were completed by all animals. Broken line: chance levels of performance. (**c**) There was also no significant effect of genotype in terms of total errors to criterion during reversal ($t < 1$; $p > 0.60$). The figure shows mean ± s.e.m. total errors to achieve a criterion of 83.3% correct choices (10 out of 12) on three consecutive days of testing.

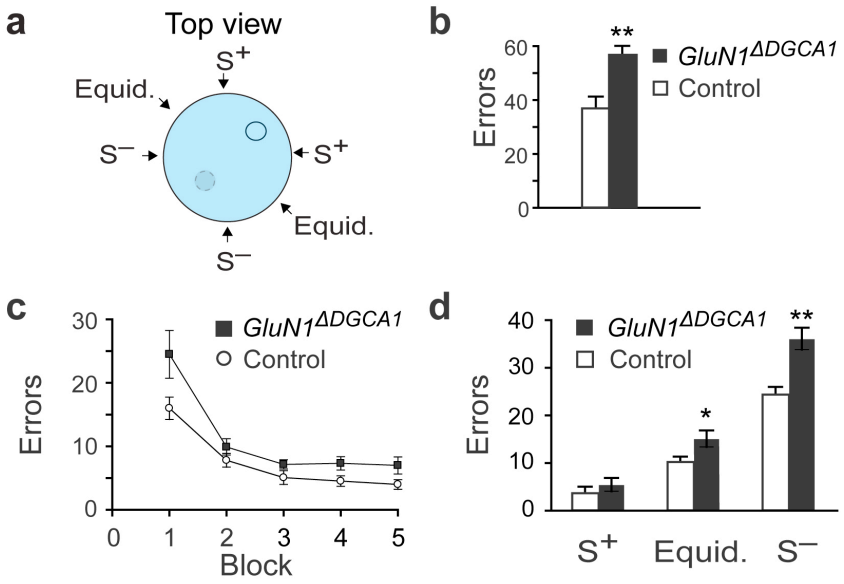

Supplementary Fig. 8. *GluN1*$^{\Delta DGCA1}$ mice are impaired on the spatial discrimination beacon task in the watermaze. (**a**) Top view of the maze gives the position of the two identical beacons and the six different starting positions. We counted the total number of errors made on a given trial. For example, if a mouse swam under the S^- beacon (dashed circled line), and then re-emerged before, again, swimming under the S^- beacon, then this was scored as two errors. Total errors data were analyzed using an ANOVA which comprised a between subjects factor of genotype (Controls vs. *GluN1*$^{\Delta DGCA1}$) and two within subjects factors; block (5 x 3 day blocks; 24 trials were required for full counterbalancing with 8 trials per day) and start position (equidistant vs. close to S^+ vs. close to S^-). **(b)** The figure shows mean ± s.e.m. total number of errors collapsed across all training blocks for Controls (n = 11) and *GluN1*$^{\Delta DGCA1}$ mice (n = 12). ANOVA revealed that the *GluN1*$^{\Delta DGCA1}$ mice made significantly more errors overall than Controls (main effect of genotype $F(1,21) = 18.53$; $p < 0.0005$). **(c)** There was also a significant reduction in the number of errors made across the 5 blocks of training, reflecting the gradual acquisition of the task ($F(4,84) = 26.61$; $p < 0.0001$), but there was no genotype by block interaction ($F(4,84) = 1.24$; $p > 0.30$). The figure shows mean ± s.e.m. number of errors per block of training (24 trials per block) in Controls and *GluN1*$^{\Delta DGCA1}$ mice. **(d)** The figure shows total errors across all training trials from the different starting positions. There was a main effect of start position ($F(2,42) = 129.76$; $p < 0.0001$), reflecting the fact that mice made more errors when starting from close to the S^- beacon and less errors when starting from close to the S^+ beacon, and, importantly, there was also a genotype by start position interaction ($F(2,42) = 5.18$; $p < 0.01$). There was also a block by start position interaction ($F(8,168) = 4.07$; $p < 0.0005$), but no genotype by block by start position triple interaction ($F < 1$; $p > 0.70$). Subsequent analysis of the genotype by start position interaction, using simple main effects, revealed that the *GluN1*$^{\Delta DGCA1}$ mice (black bars) were significantly impaired compared to Controls (white bars) on the S^- start trials ($F(1,21) = 17.02$; $p < 0.001$) and on the equidistant start trials ($F(1,21) = 5.39$; $p < 0.05$), but not on the S^+ start trials ($F < 1$; $p > 0.30$). All means ± s.e.m. Simple main effects group difference *p<0.05, **p<0.001.

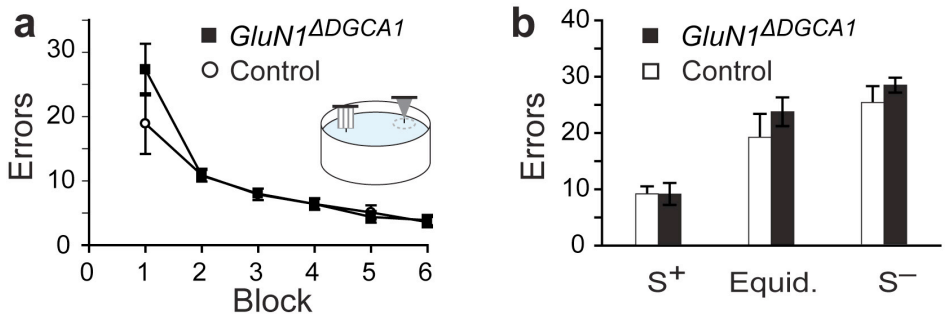

Supplementary Fig. 9. Normal performance of *GluN1*$^{\Delta DGCA1}$ mice on the non-spatial, visual discrimination beacon task in the watermaze. (a) The figure shows that there was no impairment in *GluN1*$^{\Delta DGCA1}$ mice in terms of the total errors made across 6 blocks of training (24 trials/block) on the visual discrimination beacon task. Inset: Scheme of the two visually distinct beacons in the watermaze. Only one beacon is sitting on top of the escape platform. Both Controls (n = 8) and *GluN1*$^{\Delta DGCA1}$ mice (n = 9) displayed a reduction in total errors as training proceeded. **(b)** The figure shows the total errors across all trials from different starting positions, demonstrating that all mice were less accurate at choosing the correct beacon when starting from close to the decoy beacon (S^- trials). However, there was no difference between groups for any of the start positions (8 trials/block) on this non-spatial version of the task. Data were analyzed using an ANOVA which comprised a between subjects factor of genotype (Controls vs. *GluN1*$^{\Delta DGCA1}$) and two within subjects factors; block (6 x 3 day blocks; 24 trials were required for full counterbalancing with 8 trials per day) and start position (equidistant vs. close to S^+ vs. close to S^-). There was a main effect of block ($F(5,75) = 27.71$; $p < 0.0001$), a main effect of start position ($F(2,30) = 30.74$; $p < 0.0001$), and a start position by block interaction ($F(10,150) = 4.48$; $p < 0.0001$). However, there was no main effect of genotype ($F(1,15) = 1.25$; $p > 0.20$), no genotype by block interaction ($F(5,75) = 1.67$; $p > 0.10$), no genotype by start position interaction ($F < 1$; $p > 0.50$), and no triple interaction ($F < 1$; $p > 0.90$). All means ± s.e.m.

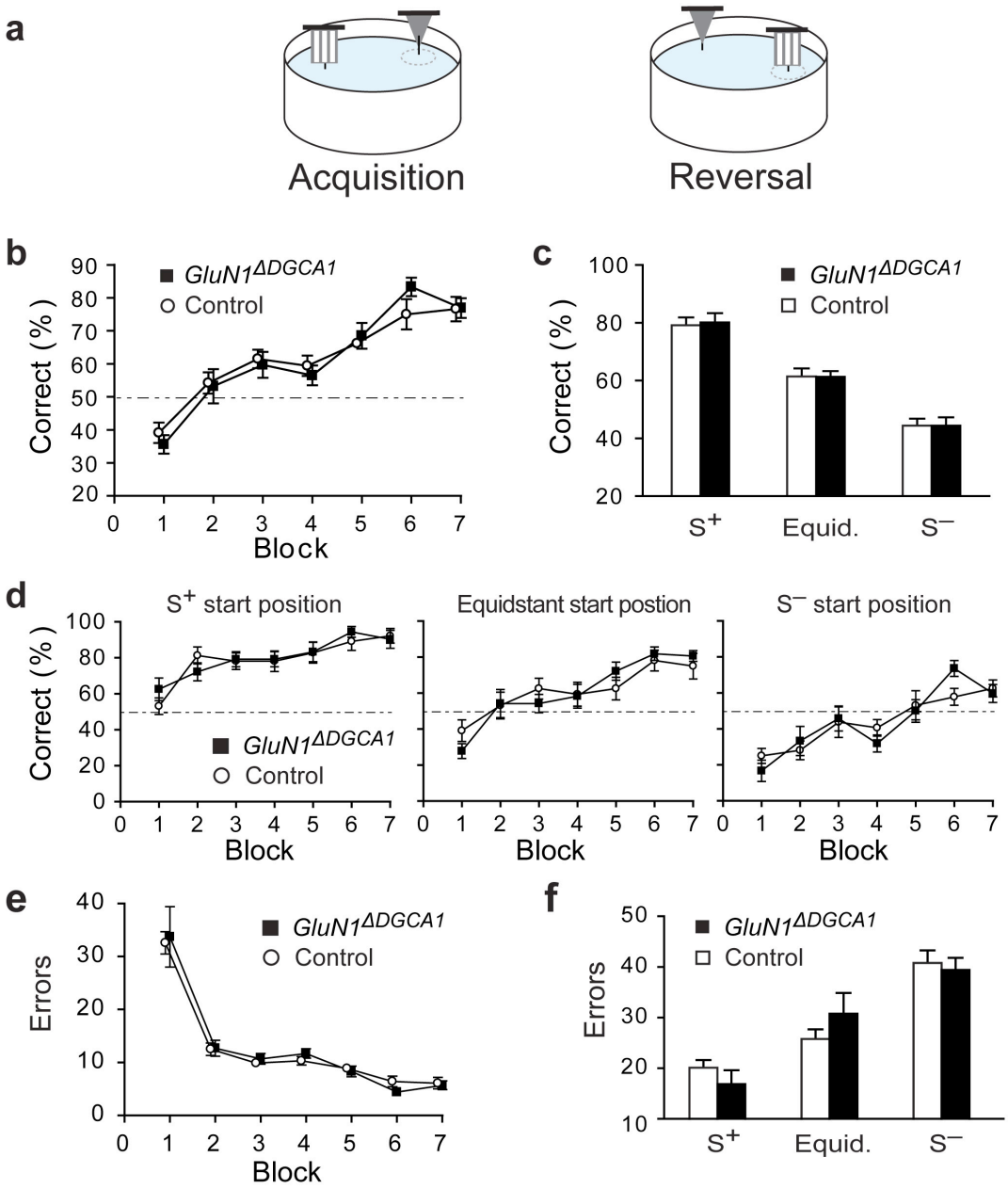

Supplementary Fig. 10. *GluN1*$^{\Delta DGCA1}$ mice are not impaired during reversal of the non-spatial, visual discrimination beacon task. **(a)** Non-spatial reversal; view of the watermaze with two visually distinct beacons. Only one beacon is sitting on top of the escape platform. Mice were first trained during Acquisition to associate a particular beacon with escape (e.g. grey funnel). Once the mice had successfully acquired the non-spatial, visual discrimination beacon task, the identities of the rewarded (+) and non-rewarded (–) beacons were reversed (Reversal). Thus, for an animal that had been trained that the grey funnel was associated with the platform during acquisition, the black and white striped cylinder was now associated with successful escape during reversal. Mice received a further 21 days of training with the platform now associated with the opposite beacon (i.e. they received 7 blocks of 24 trials per block during reversal). Testing was otherwise the same as during acquisition, with trials starting from either close to the new S^+, close to the new S^-, or equidistant between the two beacons, counterbalanced as before. Data were analyzed as previously using ANOVAs which comprised a between subjects factor of genotype (Controls vs. *GluN1*$^{\Delta DGCA1}$), and two within subjects factors; block (7 x 3 day blocks; 24 trials

were required for full counterbalancing with 8 trials per day) and start position (equidistant vs. close to S^+ vs. close to S^-). **(b)** Initially, on reversing the outcomes associated with the two visually distinct beacons, the performance of both groups of mice fell below chance levels as expected. Both groups then gradually altered their behavior so as to choose the now-rewarded (previously un-rewarded) beacon. There was no impairment in the *GluN1*$^{\Delta DGCA1}$ mice during the reversal of the non-spatial, visual discrimination beacon task. The figure shows first choice accuracy (percent correct) of both Controls (n = 8) and *GluN1*$^{\Delta DGCA1}$ mice (n = 9) improved across 7 blocks of reversal testing (24 trials/block). Broken line ,chance levels of performance. **(c)** First choice accuracy (percent correct) across all training trials from different starting positions showed that all mice were less accurate at choosing the correct beacon when starting from S^-. **(d)** The figure shows first choice accuracy (percent correct) across 7 blocks of reversal testing on trials starting from S^+, equidistant and S^- positions. There was no difference between Controls and *GluN1*$^{\Delta DGCA1}$ mice across 7 blocks of reversal testing for any of the start positions (8 trials/block). Broken line: chance levels of performance. Analysis of first choice accuracy revealed a highly significant effect of block ($F(6,90) = 43.72$; $p < 0.0001$) which reflected the gradual improvement in performance with training as the reversal phase of the experiment proceeded, and a significant main effect of start position ($F(2,30) = 121.30$; $p < 0.0001$) which reflected the fact that, not surprisingly, choice accuracy was highest on S^+ trials and lowest on S^- trials. There was no overall main effect of genotype and no significant interaction between genotype and start position (both $F < 1$; $p > 0.90$). Furthermore there were no other significant interactions involving genotype (all F's < 1.05; $p > 0.40$). (**e**) A similar pattern of results was observed in terms of total errors made. The figure shows that there was no impairment in *GluN1*$^{\Delta DGCA1}$ mice in terms of the errors made across the 7 blocks of reversal testing (24 trials/block). **(f)** The total errors across all trials from different starting positions show that all mice were less accurate at choosing the correct beacon when starting from close to the decoy beacon (S^- trials). There was no difference between Controls and *GluN1*$^{\Delta DGCA1}$ mice for any of the start positions. There was no main effect of genotype ($F < 1$; $p > 0.90$) and no genotype by start position interaction ($F(2,30) = 1.95$; $p > 0.15$). All means ± s.e.m.